

A survey of some new results in ferromagnetic thin films

Radu Ignat*

1 Introduction

Ferromagnetic materials are widely used in nowadays as technological tools, especially for magnetic data storage. The modelling of very small ferromagnetic particules is based on the micromagnetic theory. The micromagnetic model states that ferromagnetic materials can be described by a 3–D vector-field distribution, called *magnetization*, where the stable configurations correspond to (local) minimizers of the micromagnetic energy. The associated variational problem is nonconvex and nonlocal. Moreover, it is a multi-scale system involving both intrinsic parameters (depending on the nature of the ferromagnetic material) and extrinsic parameters (coming from the geometry of the sample). According to the relative smallness of these parameters, different asymptotic regimes appear and lead to the formation of various magnetization patterns.

The qualitative and quantitative analysis of the magnetization patterns is an extensively explored topic. Generically, a pattern (stable state) consists in large uniformly magnetized 3–D regions (*magnetic domains*) separated by narrow transition layers (*magnetic walls*) where the magnetization varies very rapidly. Depending on the scales of the system, the experiments predict different type of magnetic walls : 2–D wall defects (*Néel walls*, *asymmetric Bloch wall*), 1–D vortex-lines (*Bloch lines*) or a mixed type of vortex-wall defects (*cross-tie walls*). The main goal is to give a mathematical justification of the physical prediction on the formation and characterization of these defects. Classical methods of functional analysis are often insufficient to detect these phenomena of loss of regularity. New approaches need to be developed in order to implement geometric measure theory contributing to the analysis of partial differential equations.

In this survey, we focus on pattern formation in very thin films. The ferromagnetic samples are assumed to be cylinders with a very small thickness. In our regime, two types of magnetic walls are expected to be observed : Néel walls and Bloch lines. Moreover, there exists a physical prediction on global configurations of the magnetization : as stated by van den Berg [29], the observed magnetizations at the “mesoscopic” level are 2–D unit-length vector fields of distributionally vanishing divergence. A special configuration is the Landau state that corresponds to the viscosity solution of the eikonal equation. It fits perfectly to the magnetization pattern observed in experiments on rectangular thin films (see Hubert and Schafer [15]).

Our aim is to present some results that rigourously prove the van den Berg conjecture at least in a special regime. For this purpose, we discuss the properties of Néel walls and Bloch lines. These defects give the leading order term of the energy of the Landau state. The main result shows compactness of configurations energetically close to the Landau state in the case where a Bloch line is energetically more expensive than a Néel wall. Consequently, their limiting pattern satisfies the van den Berg prediction.

The paper is organized as follows : we start with a mathematical description of the 3–D micromagnetic model. Then we discuss a thin film regime where the 3–D model can be asymptotically

*Laboratoire de Mathématiques, Université Paris-Sud 11, Bât. 425, 91405 Orsay, France (e-mail: Radu.Ignat@math.u-psud.fr)

reduced to a 2–D problem. In Section 4, we introduce a toy problem that is a slight simplification of the reduced 2–D model and we explain heuristically the van den Berg prediction on the magnetization at the mesoscopic level. Next we present two models that are related with our toy problem : the Aviles-Giga model and the Rivière-Serfaty model. They appear in different asymptotic regimes in micromagnetics and exhibit the same van den Berg limiting configuration. In Section 6, we review the properties of the Néel walls, together with some new results on the optimality and Γ –convergence of these 1–D transition layers. In Section 7, we characterize the Bloch lines by analogy with vortices in Ginzburg-Landau type problems. These results enable us to deduce the energy level of the Landau state in the toy problem and to present a compactness result for magnetizations energetically close to the Landau state in Section 8.

2 The 3–dimensional model

The magnetization of a ferromagnetic sample $\Omega \subset \mathbb{R}^3$ is created by the spontaneous alignment of electron spins and can be described in the non-dimensionalized form by a unit 3–D vector field $m : \Omega \rightarrow S^2$. Let us assume that the sample is a cylinder, i.e., $\Omega = \Omega' \times (0, t)$ where Ω' is the cross section of the sample of diameter ℓ and t is the thickness of the cylinder (see FIG. 1). According

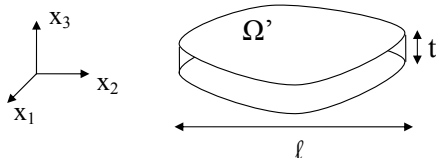


FIG. 1 – A ferromagnetic sample.

to micromagnetics, stable magnetizations on Ω are described by (local) minimizers of the energy functional defined as :

$$E^{3D}(m) = d^2 \int_{\Omega} |\nabla m|^2 dx + Q \int_{\Omega} \varphi(m) dx + \int_{\mathbb{R}^3} |\nabla U|^2 dx - 2 \int_{\Omega} H_{\text{ext}} \cdot m dx. \quad (1)$$

In the following we explain the four components of the micromagnetic energy E^{3D} .

The first term, called exchange energy is due to short range interactions of spins and favors parallel alignment of neighboring spins. The constant d is the exchange length and corresponds to an intrinsic parameter of the material on the order of nanometers.

The second term in (1) represents the anisotropy energy that penalizes certain magnetization axes. The anisotropy energy density φ is a nonnegative function with symmetry properties inherited from the crystalline lattice. The preferred directions of magnetization are the zeros of φ . Typically, we have uniaxial or multiaxial anisotropy (e.g., $\varphi(m) = 1 - m_1^2$ that favors the direction $(\pm 1, 0, 0)$) and surface anisotropy (e.g., $\varphi(m) = m_3^4$ where the easy plane is the horizontal one). The quality factor Q is a second intrinsic parameter of the material that measures the strength of the anisotropy energy relative to that of the stray field. According to the values of Q , we distinguish two classes of materials : soft materials if $Q < 1$ and hard materials if $Q > 1$.

The third term of E^{3D} is the stray field energy and is created by long range interactions between electron spins modelled by the static Maxwell equation. More precisely, the stray field potential

$U : \mathbb{R}^3 \rightarrow \mathbb{R}$ is determined by

$$\Delta U = \nabla \cdot \left(m 1_{\Omega} \right) \quad \text{in } \mathbb{R}^3, \quad (2)$$

i.e., $\int_{\mathbb{R}^3} \nabla U \cdot \nabla \zeta \, dx = \int_{\Omega} m \cdot \nabla \zeta \, dx, \quad \forall \zeta \in C_c^{\infty}(\mathbb{R}^3).$

By the electrostatic analogy, two types of charges generate the potential U : volume charges with density given by the divergence of m at the interior of the sample Ω and surface charges represented by the normal component of the magnetization on the boundary of Ω . Therefore, this nonlocal term favors domain patterns that achieve flux closure.

The last term in (1) denotes the external field energy generated by an applied external field $H_{\text{ext}} : \mathbb{R}^3 \rightarrow \mathbb{R}^3$. It favors alignment of the magnetization with the external field H_{ext} .

More details about the mathematical modelling of micromagnetics can be found in the book of Hubert and Schäfer [15] or in the overview of DeSimone, Kohn, Müller and Otto [12].

We will concentrate on the analysis of *global* minimizers of energy (1). In fact, physically accessible *local* minima share the same features as the ground state (see DeSimone, Kohn, Müller, Otto and Schäfer [13]). It is a variational problem relying on the nonconvex constraint $|m| = 1$ and the nonlocality of the stray field energy due to definition (2). On the other side, four length scales are involved in the system : two intrinsic parameters (d and Q) and two extrinsic scales (t and ℓ). The combination of nonlocality and nonconvexity with the multiscale nature of the variational problem leads to a rich pattern formation of the magnetization.

3 A reduced 2–D model

We are interested in the following thin-film regime that was studied by DeSimone, Kohn, Müller and Otto [10] : The cylinder Ω has a small aspect ratio

$$\frac{t}{\ell} \ll 1 \quad (3)$$

and the sample is large in the sense that

$$\frac{d^2}{t\ell} \ll \frac{1}{|\log \frac{\ell}{t}|}. \quad (4)$$

This regime is appropriate for permalloy films of diameter of tens of microns and thickness on the order of tens of nanometers. So, it can be achieved experimentally, though not by numerical simulation which is generally restricted to a thickness on the order of submicrons.

The main result in [10] is the reduction of the 3–D micromagnetic model to a 2–D problem by the method of Γ –convergence in the thin-film limit. In particular, the 3–D minimizers of the 3–D energy converge to configurations that only depend on the in-plane coordinates $x' = (x_1, x_2)$ and minimize a reduced 2–D energy. Here and below, the dash ' always indicates a 2–D quantity.

The reduced 2–D energy can be deduced by the following ansatz : we consider that m is invariant in the vertical variable x_3 , i.e.,

$$m = (m', m_3)(x') : \Omega' \rightarrow S^2. \quad (5)$$

In fact, because of the cylinder shape of the film and the asymptotic regime (3) & (4), the variations in the thickness direction $x_3 \in (0, t)$ are strongly penalized by the exchange energy. It is also assumed that the external field is in-plane and constant in x_3 , i.e.,

$$H_{\text{ext}} = (H'_{\text{ext}}(x'), 0).$$

The exchange energy, anisotropy and external field energy write as

$$\int_{\Omega} (d^2 |\nabla m|^2 + Q\varphi(m) - 2H_{\text{ext}} \cdot m) dx = t \int_{\Omega'} (d^2 |\nabla' m|^2 + Q\varphi(m) - 2H'_{\text{ext}} \cdot m') dx'. \quad (6)$$

What is the appropriate scaling of the stray field energy? For configurations (5), the Maxwell equation (2) turns into :

$$\Delta U = \nabla' \cdot m' 1_{\Omega} + m \cdot \nu 1_{\partial\Omega} \quad \text{in } \mathbb{R}^3, \quad (7)$$

where ν is the unit outer normal vector on $\partial\Omega$. Therefore, the volume charges are given by the in-plane flux and the surface charges on the top and the bottom side of the cylinder are represented by the out-of-plane component m_3 of the magnetization. Equation (7) is a transmission problem that can be solved explicitly using the Fourier transform $\mathcal{F}(\cdot)$ in the horizontal variables (see Appendix) and the computation yields

$$\int_{\mathbb{R}^3} |\nabla U|^2 dx = t \int_{\mathbb{R}^2} f\left(\frac{t}{2}|\xi'|\right) \left| \frac{\xi'}{|\xi'|} \cdot \mathcal{F}(m' 1_{\Omega'}) \right|^2 d\xi' + t \int_{\mathbb{R}^2} g\left(\frac{t}{2}|\xi'|\right) \left| \mathcal{F}(m_3 1_{\Omega'}) \right|^2 d\xi',$$

where

$$g(s) = \frac{1 - e^{-2s}}{2s} \quad \text{and} \quad f(s) = 1 - g(s) \quad \text{if } s \geq 0.$$

Approximating $g(s) \approx 1$ and $f(s) \approx s$ if $s = o(1)$, we obtain

$$\int_{\mathbb{R}^3} |\nabla U|^2 dx \approx \frac{t^2}{2} \int_{\mathbb{R}^2} \left| |\nabla'|^{-\frac{1}{2}} \nabla' \cdot (m' 1_{\Omega'}) \right|^2 dx' + t \int_{\Omega'} m_3^2 dx'. \quad (8)$$

Observe that the first term in (8) is related with the stray field energy associated to the following equation obtained from (7) by passing to the limit $t \downarrow 0$:

$$\Delta u = \nabla' \cdot (m' 1_{\Omega'}) \mathcal{H}^2 \llcorner \{x_3 = 0\} \quad \text{in } \mathbb{R}^3.$$

More precisely, the homogeneous $H^{-1/2}$ -seminorm of the in-plane divergence of m' is given by the Dirichlet integral of u :

$$\frac{1}{2} \int_{\mathbb{R}^2} \left| |\nabla'|^{-\frac{1}{2}} \nabla' \cdot (m' 1_{\Omega'}) \right|^2 dx' = \int_{\mathbb{R}^3} |\nabla u|^2 dx. \quad (9)$$

In order for (9) to be finite, we need to enforce vanishing charges on the lateral boundary :

$$m' \cdot \nu' = 0 \quad \text{on } \partial\Omega'.$$

For simplicity of the notation, we will think of m' as being extended to 0 outside Ω' and we will still denote this application by m' , i.e.,

$$m' := m' 1_{\Omega'}.$$

The scaling of the RHS of (6) and (8) in the length scale ℓ of Ω' is obtained by the change of variable $\tilde{x}' = x'/\ell$ ($\tilde{\Omega}' = \Omega'/\ell$), $\tilde{m}(\tilde{x}') = m(x')$ and $\tilde{H}'_{\text{ext}}(\tilde{x}') = H'_{\text{ext}}(x')$ and leads to the following 2-D approximating thin film energy :

$$E^{2D}(\tilde{m}) = t d^2 \int_{\tilde{\Omega}'} |\tilde{\nabla}' \tilde{m}|^2 d\tilde{x}' + \frac{t^2 \ell}{2} \int_{\mathbb{R}^2} \left| |\tilde{\nabla}'|^{-\frac{1}{2}} \tilde{\nabla}' \cdot \tilde{m}' \right|^2 d\tilde{x}' + t \ell^2 \int_{\tilde{\Omega}'} \left(\tilde{m}_3^2 + Q\varphi(\tilde{m}) - 2\tilde{H}'_{\text{ext}} \cdot \tilde{m}' \right) d\tilde{x}'. \quad (10)$$

This ansatz of considering x_3 -invariant magnetizations in the regime (3) & (4) is rigorously justified in [10] by the method of Γ -convergence and it explains why the energy E^{2D} is a good approximation of the 3-D functional E^{3D} .

4 A toy problem

We will discuss a simplified problem for the thin-film model presented in the previous section. We will ignore the anisotropy and the external field energy ($Q = 0$, $H_{ext} = 0$); in fact, they represent a small perturbation of the remaining terms in (10) by scaling appropriately the quality factor Q and H_{ext} . The setting of our toy problem is given in the following :

Let $\omega \subset \mathbb{R}^2$ be a planar simply connected domain with Lipschitz boundary. We focus on configurations

$$m = (m', m_3) : \omega \rightarrow S^2$$

that are tangent at the boundary, i.e.,

$$m' \cdot \nu = 0 \quad \text{on } \partial\omega, \quad (11)$$

where ν is the normal vector to $\partial\omega$. We consider the following energy functional :

$$E_{\varepsilon,\eta}(m) = \int_{\omega} |\nabla m|^2 dx + \frac{1}{\eta} \int_{\mathbb{R}^2} \left| |\nabla|^{-1/2} (\nabla \cdot m') \right|^2 dx + \frac{1}{\varepsilon^2} \int_{\omega} m_3^2 dx, \quad (12)$$

where ε and η are small positive parameters standing for the core of the Bloch line and the Néel wall, respectively (see Sections 6 and 7).

From now on, we will denote by $x = (x_1, x_2)$ the in-plane variables and by ∇ the differential operator

$$\nabla = (\partial_{x_1}, \partial_{x_2}).$$

The functional $E_{\varepsilon,\eta}$ represents the renormalization of the energy (10) by a factor $t d^2$ and the penalizing parameters correspond to $\varepsilon := \frac{d}{\ell}$ and $\eta := \frac{2d^2}{t\ell}$. The thin-film regime (3) & (4) turns into the constraint

$$\varepsilon \ll 1 \quad \& \quad \eta \ll 1. \quad (13)$$

Notice that the boundary condition (11) creates a topological obstruction for the system that enforces the existence of zeros of m' in $\bar{\omega}$. These zeros play the role of topological point-singularities (*vortices*) that carry a degree. In a 3-D bulk, they correspond to line-singularities in the vertical section, so called Bloch-lines.

Our aim is to study the limiting behavior of global minimizers of $E_{\varepsilon,\eta}$ in the regime (13). In this context, the last two terms in (12) are strongly penalized and favor charge-free configurations. This type of limiting configuration was predicted by van den Berg [29] : they are 2-D unit-length vector fields of weakly divergence-free, i.e.,

$$\begin{cases} m_3 = 0, |m'| = 1 \text{ and } \nabla \cdot m' = 0 & \text{in } \omega, \\ m' \cdot \nu = 0 & \text{on } \partial\omega. \end{cases} \quad (14)$$

We notice that the conditions in (14) are too rigid for smooth magnetization m . This can be

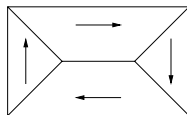


FIG. 2 – Landau state.

seen by writing $m' = \nabla^\perp \psi$ with the help of a “stream function” ψ . Here, \perp denotes an in-plane

rotation by 90° . Then (14) implies that ψ is a solution of the Dirichlet problem for the eikonal equation :

$$|\nabla\psi| = 1 \text{ in } \omega. \quad (15)$$

Using the method of characteristics, it follows that there is no smooth solution of the equation (15) in a bounded simply connected domain ω such that m' satisfies the boundary conditions (11). On the other hand, there are many continuous solutions that satisfy (15) away from a set of vanishing Lebesgue measure. One of them is the “viscosity solution” given by the distance function

$$\psi(x) = \text{dist}(x, \partial\omega)$$

that corresponds to the so-called Landau state for the magnetization m' (see FIG. 2). Hence, the divergence-free equation in (14) has to be interpreted in the distribution sense and the boundary conditions (11) are expected to induce line-singularities for solutions m' (or a point singularity in the case of a circular domain ω). These ridges (“ridges” from the point of view of ψ) are an idealization of walls in thin-film elements at the mesoscopic level. At the microscopic level, they are replaced by smooth transition layers (called Néel walls) where the magnetization varies very quickly on a small length scale. A final remark is that the normal component of m' does not jump across these discontinuity lines (because of (14)) and therefore, the normal of the mesoscopic wall is determined by the angle between the mesoscopic levels in the adjacent domains (see FIG. 3).

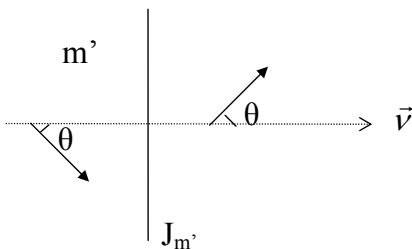


FIG. 3 – Angle wall.

We expect that the leading order term of the energy of the Landau state is given by the cost of line and point defects. Therefore, we analyse the qualitative and quantitative behavior of the Néel walls and Bloch-lines in Sections 6 and 7. This study allows us to state a compactness result for the Landau state in Theorem 4 and to conclude that the limiting configurations in that regime satisfy the van den Berg prediction.

5 Two related problems

Let us compare the toy problem with two related singularly perturbed variational problems. The first one was raised by Aviles and Giga [4] in connection with several physical applications (smectic liquid crystals, film blisters or convective pattern formation) and it was intensively studied since then, e.g. by Ambrosio, DeLellis and Mantegazza [3], DeSimone, Kohn, Müller and Otto [9], Jin and Kohn [20] etc. It consists in minimizing the energy functional

$$\begin{cases} AG_\varepsilon(m') = \int_\omega \left(\varepsilon |\nabla m'|^2 + \frac{1}{\varepsilon} (1 - |m'|^2)^2 \right) dx, \\ m'(x) : \omega \subset \mathbb{R}^2 \rightarrow \mathbb{R}^2, \quad \nabla \cdot m' = 0 \text{ in } \omega, \end{cases} \quad (16)$$

or more generally, in studying 2–D divergence-free vector fields $\{m'_\varepsilon\}$ with uniformly bounded energy $AG(m'_\varepsilon) \leq C$ as $\varepsilon \downarrow 0$. With respect to (12), the vector fields are constrained to be of divergence-free in problem (16); they will tend to be of length 1 as $\varepsilon \downarrow 0$.

The second problem was considered by Rivière and Serfaty [26, 27] and Alouges, Rivière and Serfaty [2] as a model for x_3 –invariant magnetizations in thicker films with strong planar anisotropy. It consists in reversing the limiting processes in (16), i.e., the vector fields are restricted to be of unit length and they are no longer of divergence-free, but the latter condition is forced by a penalization in the H^{-1} –norm as $\varepsilon \downarrow 0$:

$$\begin{cases} RS_\varepsilon(m') = \int_\omega \varepsilon |\nabla m'|^2 dx + \frac{1}{\varepsilon} \int_{\mathbb{R}^2} ||\nabla|^{-1} \nabla \cdot (m' \mathbf{1}_\omega)|^2 dx, \\ m'(x) : \omega \subset \mathbb{R}^2 \rightarrow \mathbb{R}^2, \quad |m'| = 1 \text{ in } \omega. \end{cases} \quad (17)$$

Observe that the first problem (16) is local, whereas (17) has a nonlocal behavior due to the last term of the energy RS_ε . Therefore, the feature of (17) is much closer to our toy problem. However, the boundary condition (11) cannot stand true for problem (17). Indeed, there are no $H^1(\omega, S^1)$ –vector fields with values into the unit circle that are tangent at the boundary of a simply connected domain ω . On the other hand, (11) is strongly penalized by the second term in the energy RS_ε as $\varepsilon \downarrow 0$.

As in the toy problem, the limiting configurations in (16) and (17) will satisfy as $\varepsilon \downarrow 0$:

$$\nabla \cdot m' = 0 \quad \text{and} \quad |m'| = 1 \quad \text{in } \omega.$$

In fact, compactness results for sequences $\{m'_\varepsilon\}$ of uniformly bounded energy are proved for problem (16) in [3] and [9], respectively for problem (17) in [26, 27]. The accumulation points are indeed 2–D unit-length vector fields of weakly divergence free. Therefore, we expect to have line-singularities for solutions m' in the limit $\varepsilon \downarrow 0$ and the normal component m'_ν of m' does not jump across these ridges.

However, the Γ –limit energies for these functionals have different behavior. In fact, the energetic cost on a ridge $J_{m'}$ can be computed by considering 1–D transition layers that connect two directions of angle $-\theta$ and θ with $\theta \in (0, \pi/2]$ (see FIG. 3). In the first model (16), the divergence-free constraint enforces that the normal component of the 1–D transition layer across the ridge is constant. Therefore, the associated variational problem can be expressed in terms of the tangential component m_τ and corresponds to a Cahn-Hilliard type model :

$$\begin{cases} AG_\varepsilon^{1D}(m_\tau) = \int_{\mathbb{R}} \left(\varepsilon \left| \frac{dm_\tau}{dt} \right|^2 + \frac{1}{\varepsilon} (\sin^2 \theta - m_\tau^2)^2 \right) dt, \\ m_\tau : \mathbb{R} \rightarrow [-\sin \theta, \sin \theta] \text{ and } m_\tau(\pm\infty) = \pm \sin \theta. \end{cases}$$

The energy AG_ε^{1D} is invariant under translation. Since configurations m_τ of finite energy are continuous, the limit conditions enforce a zero (transition wall) for m_τ and one can fix the center of the wall at the origin by setting $m_\tau(0) = 0$. The minimizer m_τ of AG_ε^{1D} is unique and satisfies the Cauchy problem associated to the first order ODE (see [20]) :

$$\frac{dm_\tau}{dt} = \frac{1}{\varepsilon} (\sin^2 \theta - m_\tau^2), \quad m_\tau(0) = 0.$$

Therefore, it is a transition layer with a single length scale ε , i.e.,

$$m_\tau(t) = \sin \theta \tanh\left(\frac{t \sin \theta}{\varepsilon}\right)$$

and satisfies the limit conditions $m_\tau(\pm\infty) = \pm \sin \theta$. The minimal energy is equal to

$$\min AG_\varepsilon^{1D} = \frac{8}{3} |\sin \theta|^3 = \frac{1}{3} |m^+ - m^-|^3,$$

where $m^\pm = (\cos \theta, \pm \sin \theta)$ are the traces of the magnetization on the ridge $J_{m'}$.

Let us now compute the cost of the Γ -limit of $\{RS_\varepsilon\}$ on the ridge $J_{m'}$ for the second model (17). Since the transition layer is of length 1, we transpose the corresponding variational problem in terms of the phase (*lifting*) φ of m' (see [26]) :

$$\begin{cases} RS_\varepsilon^{1D}(\varphi) = \int_{\mathbb{R}} \left(\varepsilon \left| \frac{d\varphi}{dt} \right|^2 + \frac{1}{\varepsilon} (\cos \varphi - \cos \theta)^2 \right) dt, \\ \varphi : \mathbb{R} \rightarrow [-\theta, \theta] \text{ and } \varphi(\pm\infty) = \pm\theta. \end{cases}$$

As before, since the energy RS_ε^{1D} is invariant under translation, we fix the center of the phase transition at the origin by setting $\varphi(0) = 0$. The minimizer φ of RS_ε^{1D} is unique and satisfies the Cauchy problem associated to the first order ODE (see [26]) :

$$\frac{d\varphi}{dt} = \frac{1}{\varepsilon} (\cos \varphi - \cos \theta), \quad \varphi(0) = 0.$$

It is an increasing transition layer with a single length scale ε that satisfies the limit conditions $\varphi(\pm\infty) = \pm\theta$ and the minimal energy is equal to

$$\min RS_\varepsilon^{1D} = 2 \int_{\mathbb{R}} (\cos \varphi - \cos \theta) \frac{d\varphi}{dt} dt = 4(\sin \theta - \theta \cos \theta).$$

Remark : The energetic cost (per unit length) of a jump across a ridge of angle 2θ is cubic ($\approx \theta^3$) in both models (16) and (17) for small angles θ . However, for large angles θ , the Γ -limit energy charges differently a jump in (16) and (17).

6 Néel walls

The Néel wall is a dominant transition layer in thin ferromagnetic films. It is characterized by a one-dimensional in-plane rotation connecting two (opposite) directions of the magnetization (see FIG. 3) :

$$m_3 = 0 \quad \text{and} \quad m = m(x_1).$$

It is a two length scale object : a small core with fast varying rotation and two logarithmically decaying tails. There are three confining mechanisms for the Néel tails : the anisotropy of the material, the steric interaction with the sample edges and the steric interaction with the tails of neighboring Néel walls. These models correspond to three nonconvex and nonlocal variational problems depending on a small parameter (see Ignat [16]).

For simplicity, here we only describe the case of confining tails by the finite size of the sample. The constraints are given by :

$$m' = (m_1, m_2) : \mathbb{R} \rightarrow S^1 \text{ and } m'(\pm x_1) = \begin{pmatrix} \alpha \\ \pm \sqrt{1 - \alpha^2} \end{pmatrix} \text{ for } \pm x_1 \geq 1, \quad (18)$$

with $\alpha \in [0, 1)$ (see FIG. 4). Denoting $\theta = \arccos \alpha$, then 2θ is called the Néel wall angle. For configurations (18), the energy (12) per unit length in x_2 -direction turns into :

$$E_\eta^{1D}(m') = \int_{\mathbb{R}} \left| \frac{dm'}{dx_1} \right|^2 dx_1 + \frac{1}{\eta} \int_{\mathbb{R}} \left| \left| \frac{d}{dx_1} \right|^{1/2} m_1 \right|^2 dx_1. \quad (19)$$

Under these restrictions, a Néel wall corresponds to a minimizer of energy (19).

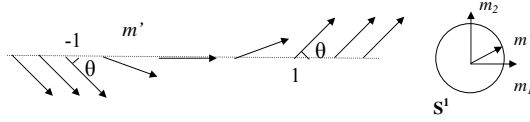


FIG. 4 – Néel wall of angle 2θ confined in $[-1, 1]$.

Notice that the continuous transition layers are necessarily not charge-free, i.e.,

$$\nabla \cdot m' = \frac{dm_1}{dx_1} \neq 0.$$

Hence there is a competition between the first and second term in (19). The main feature of the variational problem is that the renormalized energy ηE_η^{1D} only gives uniform bound of m_1 in $\dot{H}^{1/2}(\mathbb{R})$ that barely fails to control the $L^\infty(\mathbb{R})$ -norm $\|m_1\|_{L^\infty(\mathbb{R})} = 1$. This suggests a logarithmic singular behavior. The prediction of the logarithmic scaling for minimal energies ηE_η^{1D} was formally proved by Riedel and Seeger [25]; a detailed mathematical discussion of their results was carried out by Garcia-Cervera [14] by means of a perturbation argument. The exact leading order term of the minimal energy was finally deduced by DeSimone, Kohn, Müller and Otto [8, 11] by matching upper and lower bounds in the case of a 180° Néel wall, i.e., $\alpha = 0$:

$$\min_{\substack{(18) \\ \alpha=0}} E_\eta^{1D} \approx \frac{\pi}{\eta |\log \eta|} \quad \text{as } \eta \downarrow 0. \quad (20)$$

The analysis of the structure of a minimizer of (20) is rather subtle due to the different scaling behavior of the energy terms in (19). This suggests the existence of two length scales of the transition layer. The Néel wall is divided in two regions : a core ($|t| \lesssim w_{core}$) and two tails ($w_{core} \lesssim |t| \lesssim w_{tail}$). This particular structure enables the magnetization to decrease the renormalized energy ηE_η^{1D} by a logarithmic factor (20). Melcher [22, 23] rigorously established the optimal profile of the Néel wall, i.e., the minimizer m' of (20) with $m_1(0) = 1$ is unique and exhibits two uniform logarithmic tails beyond a core region of order η close to the origin (see FIG. 5 and FIG. 6) :

$$m_1(t) \sim \frac{|\log |t||}{|\log \eta|} \quad \text{for } \eta < |t| \ll 1.$$

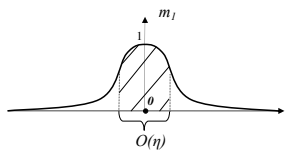


FIG. 5 – First component of a 180° Néel wall.

The stability of 180° Néel walls under arbitrary 2–D modulation was proved by DeSimone, Knüpfer and Otto [7]. The setting is the following : We consider the cross section of the thin ferromagnetic sample as a 2–D sheet $\omega = (-1, 1) \times \mathbb{R}$. The admissible magnetizations are 2–D unit-length vector fields

$$m' = (m_1, m_2) : \mathbb{R}^2 \rightarrow S^1$$

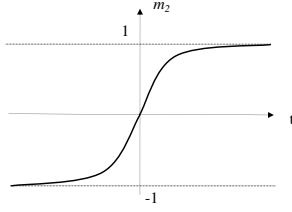


FIG. 6 – Second component of a 180° Néel wall.

that satisfy the boundary conditions in (18) and m' is L -periodic in the infinite x_2 -direction, i.e.,

$$m'(x_1, x_2 + L) = m'(x_1, x_2), \forall (x_1, x_2) \in \mathbb{R}^2 \text{ and } m'(\pm x_1, x_2) = \begin{pmatrix} \alpha \\ \pm\sqrt{1 - \alpha^2} \end{pmatrix}, \forall x_2 \in \mathbb{R}, \pm x_1 \geq 1, \quad (21)$$

where L is an arbitrary positive number. These magnetizations macroscopically connect two directions which form an angle (see FIG. 7). Then the energy density (12) for this configuration

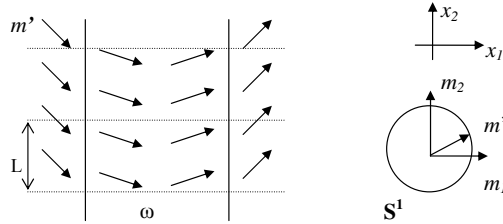


FIG. 7 – The admissible magnetization m'

writes

$$E_\eta^{per}(m') = \int_{\mathbb{R} \times [0, L]} |\nabla m'|^2 dx + \frac{1}{\eta} \int_{\mathbb{R} \times [0, L] \times \mathbb{R}} \left| |\nabla|^{-1/2} (\nabla \cdot m') \right|^2 dx. \quad (22)$$

The stability result for the 180° Néel wall in [7] is stated as follows :

$$\min_{\substack{m'=m'(x_1, x_2) \text{ with (21)} \\ |m'|=1, \alpha=0}} E_\eta^{per}(m') \approx \min_{\substack{m'=m'(x_1) \text{ with (18)} \\ \alpha=0}} E_\eta^{per}(m') \approx \frac{\pi L}{\eta |\log \eta|} \text{ as } \eta \downarrow 0.$$

This means that asymptotically, the minimal energy E_η^{per} is assumed by a straight wall. More precisely, the variations of the optimal 1-D transition layer in x_2 -direction will not decrease the leading order term in the energy.

Later, Ignat and Otto[17] showed a qualitative property of the optimal 1-D transition layers : asymptotically, the minimal energy can be attained *only* by the straight walls. This property holds for general boundary conditions (21). It is based on a compactness result for in-plane unit-length magnetizations with energies close to the minimal energy level : Any accumulation limit m^* has its singularities concentrated on a vertical line (see FIG. 8).

Theorem 1 (Ignat and Otto [17]) *Let $\alpha \in [0, 1)$ and $L > 0$ be given. For any $\delta > 0$ there exists $\eta_0 > 0$ with the following property : Given $m' : \mathbb{R}^2 \rightarrow S^1$ such that (21) holds and*

$$\eta |\log \eta| E_\eta^{per}(m') \leq L\pi(1 - \alpha)^2 + \eta_0, \quad \text{for some } 0 < \eta \leq \eta_0,$$

then we have

$$\int_{\mathbb{R} \times [0, L)} |m' - m^*| dx \leq \delta,$$

where m^* is a straight wall given by

$$m^*(x_1, x_2) = \begin{pmatrix} \alpha \\ \pm \sqrt{1 - \alpha^2} \end{pmatrix} \text{ for } \pm x_1 > \pm x_1^*, \quad (23)$$

for some $x_1^* \in [-1, 1]$.

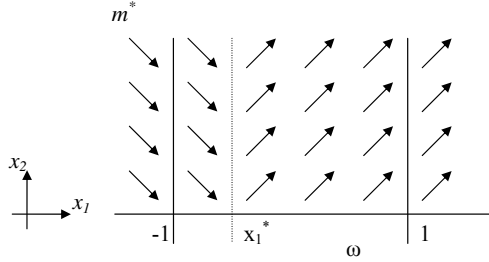


FIG. 8 – Straight wall

A natural question about the Γ -convergence for the Néel walls arises in this framework. Due to (20), we consider a new length scale $\delta > 0$ such that $\eta = \delta/|\log \delta|$ and we renormalize the energy (19) by a factor $\eta |\log \delta|$ in order for the minimal energy to become of order $O(1)$:

$$\tilde{E}_\delta(m') = \delta \int_{\mathbb{R}} \left| \frac{dm'}{dx_1} \right|^2 dx_1 + |\log \delta| \int_{\mathbb{R}} \left| \left| \frac{d}{dx_1} \right|^{1/2} m_1 \right|^2 dx_1. \quad (24)$$

The goal is to study the Γ -limit of energies $\{\tilde{E}_\delta\}$ as $\delta \downarrow 0$ and to characterize the limiting configurations of the magnetization.

The compactness result of configurations of uniformly bounded energy $\{\tilde{E}_\delta\}_{\delta \downarrow 0}$ is given in the following :

Theorem 2 (Ignat and Otto[17], Ignat [16]) *Let $\delta_k \downarrow 0$ as $k \uparrow \infty$, $\alpha_k \in [-1, 1]$ and $m'_k = (m_{1,k}, m_{2,k}) : \mathbb{R} \rightarrow S^1$ be such that (18) holds and*

$$\limsup_{k \uparrow \infty} \tilde{E}_{\delta_k}(m'_k) < +\infty. \quad (25)$$

Then $\{m'_k\}_{k \uparrow \infty}$ is relatively compact in $L^1_{loc}(\mathbb{R}, S^1)$. Any accumulation point $m' : \mathbb{R} \rightarrow S^1$ is of bounded total variation and can be written as

$$m' = \sum_{n=1}^{N+1} \begin{pmatrix} \cos \theta \\ (-1)^n \sin \theta \end{pmatrix} 1_{(t_{n-1}, t_n)}, \quad (26)$$

where $\theta \in [0, 2\pi)$, $N \geq 0$ and $-\infty < t_0 < -1 \leq t_1 < \dots < t_N \leq 1 < t_{N+1} = +\infty$. Moreover, if $\sin \theta \neq 0$, then N is an odd integer and m' satisfies (18).

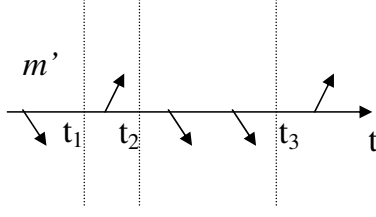


FIG. 9 – A limit configuration with 3 walls.

Remark :

- i) The limiting configurations exhibit a finite number of walls of identical angle 2θ . All these walls are confined in $[-1, 1]$ because of the boundary condition (18).
- ii) Observe that the initial configurations $\{m'_k\}$ satisfy boundary conditions (18) determined by different numbers $\{\alpha_k\}$. The angle of the limit configuration m' represents an accumulation point of the sequence $\{2 \arccos \alpha_k\}$.
- iii) The fading \dot{H}^1 -control of the magnetization is essential for the compactness result. In the absence of it, we can construct a sequence of magnetizations $\{m'_k\}$ that satisfy (18), $\|m_{1,k}\|_{\dot{H}^{1/2}} \rightarrow 0$ as $k \uparrow \infty$ and $\{m'_k\}$ is not relatively compact in L^1_{loc} (see [16]).
- iv) The compactness result in Theorem 2 fails in general in the BV_{loc} -topology even if the limiting configurations are of bounded variation in \mathbb{R} . In fact, Ignat and Otto [17] constructed a sequence of magnetizations $\{m'_k\}$ with (18) and of uniformly bounded energy $\tilde{E}_{\delta_k}(m'_k) \leq C$ such that the sequence of total variations $\{\int_{\mathbb{R}} |\frac{dm_{1,k}}{dt}|\}$ blows-up.

Let us denote by \mathcal{A} the set of all limiting configurations given by (26). For such a configuration $m' \in \mathcal{A}$, we define the following energy :

$$\tilde{E}_0(m') = \pi(1 - |m_1|)^2 \cdot \left(\text{number of jumps of } m' \right),$$

where the number N of jumps of m' corresponds to the number of straight walls of the limiting magnetization m' . We can show that \tilde{E}_0 represents the Γ -limit of energies \tilde{E}_δ as $\delta \downarrow 0$:

Theorem 3 (Ignat [16]) *Let $\delta_k \downarrow 0$ as $k \uparrow \infty$. Then*

$$\tilde{E}_{\delta_k} \xrightarrow{\Gamma} \tilde{E}_0 \text{ under the } L^1_{loc}(\mathbb{R}, S^1)\text{-topology as } k \uparrow \infty, \text{ i.e.,}$$

- (i) *If $m'_k : \mathbb{R} \rightarrow S^1$ and $\alpha_k \in [-1, 1]$ are such that (18) and (25) hold and $m'_k \rightarrow m'$ in $L^1_{loc}(\mathbb{R}, S^1)$, then $m' \in \mathcal{A}$ and*

$$\liminf_{k \uparrow \infty} \tilde{E}_{\delta_k}(m'_k) \geq \tilde{E}_0(m');$$

- (ii) *For every $m' \in \mathcal{A}$, there exist smooth functions $m'_k : \mathbb{R} \rightarrow S^1$ such that $m'_k = m'$ in $\mathbb{R} \setminus [-1, 1]$, $m'_k - m' \rightarrow 0$ in $L^1(\mathbb{R}, \mathbb{R}^2)$ and*

$$\lim_{k \uparrow \infty} \tilde{E}_{\delta_k}(m'_k) = \tilde{E}_0(m').$$

Remark : Our result yields that the energy of a Néel wall is quartic in θ for a small angle 2θ :

$$\min_{(18)} \tilde{E}_\delta \stackrel{\delta \downarrow 0}{\approx} \pi(1 - |\cos \theta|)^2 \approx \frac{\pi}{4} \theta^4 \quad \text{as } \theta \downarrow 0.$$

Observe the difference between models (16) and (17) where the limit energy charges a jump across a ridge of angle 2θ as a cubic power θ^3 for small angles θ . Therefore, the Γ -convergence for Néel walls is rather non-standard because the optimal profiles of the phase-transitions in (24) have a logarithmic tail, and thus the competition between the two terms of the energy \tilde{E}_δ is uneven. In particular, the method of “entropies” used in [20] and [9] does not work for this problem. The idea is to use a logarithmically failing interpolation inequality. For the compactness of magnetizations $\{m'_k\}$ in Theorems 2, we need to control in some sense their variations which consists in studying the derivatives of the first components $\{\sigma_k := \frac{dm_{1,k}}{dt}\}$. The energy controls the homogeneous $\dot{H}^{-1/2}$ -seminorm of σ_k in the regime $O(\frac{1}{|\log \delta_k|})$. The idea is to use a duality argument by estimating the product

$$\langle \chi_k, \sigma_k \rangle_{\dot{H}^{1/2}, \dot{H}^{-1/2}}$$

for a trial function χ_k that counts the variations of $m_{1,k}$. Therefore, it is enough to analyse the rate of the failing interpolation embedding

$$BV \cap L^\infty(\mathbb{R}) \not\subseteq \dot{H}^{1/2}(\mathbb{R})$$

that corresponds to the failing Gagliardo-Nirenberg type inequality :

$$\int \left| \left| \frac{d}{dt} \right|^{1/2} \chi_k \right|^2 \not\lesssim \sup |\chi_k| \int \left| \frac{d\chi_k}{dt} \right|. \quad (27)$$

Typically, the trial function χ_k has jumps so that $\chi_k \notin \dot{H}^{1/2}(\mathbb{R})$. That can be corrected by using a perturbation of the homogeneous $\dot{H}^{1/2}$ -seminorm that gives a weaker seminorm as in the work of DeSimone, Knüpfer and Otto [7]. This seminorm is controlled by the RHS term in (27) by a logarithmically slow rate with an optimal prefactor $\frac{2}{\pi}$. This optimal factor gives the exact leading order term of the energy (20).

7 Bloch line

A Bloch line is a smooth 3-D structure on the microscopic level of the magnetization that replaces a topological point singularity at the mesoscopic level. The prototype of a Bloch line is given by a vector field

$$m : \omega \rightarrow S^2$$

that is defined in a circular cross-section $\omega := B_1 \subset \mathbb{R}^2$ of a film and satisfies :

$$\nabla \cdot m' = 0 \text{ in } B_1 \text{ and } m'(x) = x^\perp \text{ on } \partial B_1. \quad (28)$$

Here, the Bloch line is assumed to be invariant in the vertical direction and the word “line” refers to that direction. The magnetization turns in-plane at the boundary of the disk B_1 . Therefore, the in-plane component m' looks like a regularization of a vortex $x^\perp/|x|$. This topological constraint creates a localized region, the core of the Bloch line, where the magnetization becomes perpendicular to the horizontal plane (see FIG. 10). The out-of-plane component m_3 represents the surface charges. Compared to Néel walls, the Bloch line is a configuration that avoids volume charges.

The energy (12) for a magnetization (28) writes as :

$$E_{\varepsilon,\eta}(m) = \int_{B_1} |\nabla m|^2 dx + \frac{1}{\varepsilon^2} \int_{B_1} m_3^2 dx. \quad (29)$$

The Bloch line corresponds to the minimizer of (29) under the constraint (28). Observe that the competition between the exchange and the stray field energy (by the penalization of surface

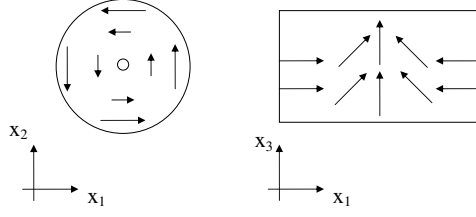


FIG. 10 – Bloch line.

charges) yields that the size of the core of the Bloch line is of order ε . Since $|\nabla m'| \leq |\nabla m|$ and $1 \geq m_3^2 \geq m_3^4 = (1 - |m'|^2)^2$, (29) has a lower bound given by the following Ginzburg-Landau type functional :

$$GL_\varepsilon(m') = \int_{B_1} |\nabla m'|^2 dx + \frac{1}{\varepsilon^2} \int_{B_1} (1 - |m'|^2)^2 dx.$$

The theory developed in the book of B ethuel, Brezis and H elein [5] shows that the minimal energy GL_ε under the restriction that m' has winding number 1 is of order $|\log \varepsilon|$:

$$\min_{\substack{m' \in H^1(B_1, \mathbb{R}^2) \\ m' = x^\perp \text{ on } \partial B_1}} GL_\varepsilon(m') \approx 2\pi |\log \varepsilon| \text{ as } \varepsilon \downarrow 0.$$

Moreover, Riviere and Pacard [24] proved that the minimizer of GL_ε is unique and radially symmetric around the origin for a sufficiently small $\varepsilon > 0$, i.e.,

$$m'(x) = f(|x|) \frac{x^\perp}{|x|}, \quad (30)$$

where the profile f is the unique solution of the following Cauchy problem associated to a second order ODE :

$$\begin{cases} -\frac{d^2 f}{dr^2} - \frac{1}{r} \frac{df}{dr} + \frac{f}{r^2} = \frac{2}{\varepsilon^2} f(1 - f^2) \text{ in } (0, 1), \\ f(0) = 0, f(1) = 1. \end{cases}$$

Also notice that the minimizer (30) of GL_ε is divergence-free, hence it satisfies (28).

An upper bound for our energy (29) can be deduced by computing the energetic level of the configuration

$$\tilde{m}'(x) = \tilde{f}(|x|) \frac{x^\perp}{|x|}, \quad \tilde{m}_3 = \sqrt{1 - |\tilde{m}'|^2} \text{ with } \tilde{f}(r) = \begin{cases} \sin(\frac{\pi r}{2\varepsilon}) & \text{if } r \in (0, \varepsilon), \\ 1 & \text{if } r \in (\varepsilon, 1). \end{cases}$$

Then \tilde{m}' satisfies (28) and we have for $\varepsilon < 1$,

$$E_{\varepsilon, \eta}(\tilde{m}') \leq 2\pi |\log \varepsilon| + C,$$

where C is some positive constant.

Therefore, we conclude that

$$E_{Bloch} \approx 2\pi |\log \varepsilon| \text{ as } \varepsilon \downarrow 0.$$

8 Compactness of the Landau state

We are now able to estimate the energy of the Landau state. The Landau state is a smooth structure at the microscopic level whose in-plane component replaces the viscosity solution $m' = \nabla^\perp \psi$ associated to the problem (14) at the mesoscopic level where the stream function is $\psi = \text{dist}(x, \partial\omega)$. As explained in Section 4, ψ generates ridges (line-defects) that turn into Néel walls for the Landau state. Also, the Landau state presents point-defects corresponding to Bloch lines. The existence of a Bloch line is enforced by the topological constraint involved in the boundary condition (11). Therefore, we expect that the energy of the Landau state is of the following leading order :

$$E_{\text{Landau}} \approx 2\pi |\log \varepsilon| + \frac{A}{\eta |\log \eta|},$$

where ε and η are the sizes of the core of the Bloch line and the Néel wall, respectively. Here, A is a positive constant depending on the angle and length of the Néel walls.

In the regime where ε is exponentially small with respect to η , we prove the compactness of 3–D magnetizations that are energetically close to the Landau state. Consequently, the limit configurations do satisfy the van den Berg prediction.

Theorem 4 (Ignat and Otto [18]) *Let $\omega \subset \mathbb{R}^2$ be a smooth simply connected domain and let $A > 0$ and $\alpha \in (0, 1/2)$ be two arbitrary constants. Let $\varepsilon_k, \eta_k > 0$, $k \in \mathbb{N}$ be two sequences such that*

$$\frac{A}{\eta_k |\log \eta_k|} \leq 2\pi\alpha |\log \varepsilon_k| \text{ for every } k \in \mathbb{N} \quad (31)$$

and

$$\varepsilon_k \downarrow 0, \eta_k \downarrow 0 \quad \text{as } k \uparrow \infty.$$

If $m_k : \omega \rightarrow S^2$ are C^1 functions satisfying (11) and

$$E_{\varepsilon_k, \eta_k}(m_k) \leq 2\pi |\log \varepsilon_k| + \frac{A}{\eta_k |\log \eta_k|}, \quad (32)$$

then $\{m_k\}_{k \uparrow \infty}$ is relatively compact in $L^1(\omega)$ and any accumulation point $m : \omega \rightarrow S^2$ satisfies

$$m_3 = 0, |m'| = 1 \text{ a.e. in } \omega \quad \text{and} \quad \nabla \cdot m' = 0 \text{ distributionally in } \omega. \quad (33)$$

The compactness result in Theorem 4 is based on the approximation of 3–D configurations by unit 2–D vector fields away from a small region. That region is detected via the following theorem. It comes by using some topological techniques due to Jerrard [19] and Sandier [28] for the concentration of the Ginzburg-Landau energy around vortices (see also Lin [21]). In our regime (31), the level of energy (32) supports only one interior vortex or it concentrates on the boundary (when boundary vortices do exist).

Theorem 5 (Ignat and Otto [18]) *We consider $\omega \subset \mathbb{R}^2$ be a smooth simply connected domain. Let $\sigma > 0$, $\alpha \in (0, 1/2)$ and $m' : \omega \rightarrow \mathbb{R}^2$ be a C^1 function satisfying (11). Then there exists $\varepsilon_0 > 0$ such that the condition*

$$\int_{\omega} GL_{\varepsilon}(m') dx \leq 2\pi(1 + \alpha) |\log \varepsilon| \quad \text{for } 0 < \varepsilon \leq \varepsilon_0 \quad (34)$$

imply either the existence of a vortex ball $B(x^*, \sigma) \subset \omega$ with

$$\int_{B(x^*, \sigma)} GL_{\varepsilon}(m') dx \geq 2\pi \left| \log \frac{\sigma}{\varepsilon} \right| - C(\alpha),$$

or the following lower estimate of the energy at the boundary $\partial\omega$:

$$\int_{\{x \in \omega : \text{dist}(x, \partial\omega) < \sigma\}} GL_\varepsilon(m') dx \geq 2\pi \left| \log \frac{\sigma}{\varepsilon} \right| - C(\alpha).$$

In Theorem 5, a small region is detected where $GL_{\varepsilon_k}(m'_k)$ is concentrated : either a disk of radius σ or a band of width σ near the boundary $\partial\omega$. Let us denote this region by ω_σ . Away from ω_σ , the energy level (32) only allows line singularities. Fix a disk \mathcal{D} inside $\omega \setminus \omega_\sigma$. One can detect a square grid in the interior of the disk with the following properties : each cell has a small size, $|m'_k| \geq 1/2$ on the grid and the degree of m'_k vanishes on the boundary of each cell of the grid. Thus, m'_k can be approximated by a unit 2-D vector field v_k in the interior of \mathcal{D} and v_k has the same level of energy $O(\frac{1}{\eta_k |\log \eta_k|})$ as m'_k in \mathcal{D} . The following compactness result for 2-D configurations applies and the conclusion of Theorem 4 follows immediately.

Theorem 6 (Ignat and Otto[17]) *Consider a sequence $\{\eta_k\}_{k \in \mathbb{N}} \subset (0, \infty)$ with $\eta_k \downarrow 0$ and for $k \in \mathbb{N}$, let $v_k : B_1 \subset \mathbb{R}^2 \rightarrow S^1$. Suppose that*

$$\limsup_{k \rightarrow \infty} \eta_k |\log \eta_k| \left(\int_{B_1} |\nabla v_k|^2 dx + \frac{1}{\eta_k} \int_{B_1} ||\nabla|^{-1/2} (\nabla \cdot v_k)|^2 dx \right) < \infty.$$

Then $\{v_k\}_{k \uparrow \infty}$ is relatively compact in $L^1(B_1)$ and any accumulation point $v : B_1 \rightarrow \mathbb{R}^2$ satisfies

$$|v| = 1 \text{ a.e. in } B_1 \quad \text{and} \quad \nabla \cdot v = 0 \text{ distributionally in } B_1. \quad (35)$$

Theorem 6 is the generalization of Theorem 2 for 2-D magnetizations. The proof uses a localized version of the interpolation-type inequality that is explained in the last remark in Section 6. The idea is to control the length of an orbit of the flow v_k^\perp as in the work of DeSimone, Knüpfer and Otto [7]. In fact, such an orbit corresponds to a flow line of v^\perp in the limit $k \uparrow \infty$, which is a straight characteristic in the case of a smooth solution v of (35). If χ_k is a characteristic function with the jump set concentrated on an orbit of v_k^\perp and ρ is a cut-off function, then the localized “duality” term $\langle \chi_k, \nabla \cdot v_k \rangle_{\dot{H}^{1/2}, \dot{H}^{-1/2}}$, i.e.,

$$\int \rho \chi_k \nabla \cdot v_k dx$$

controls the local length $\int \rho |\nabla \chi_k| dx$ of the orbit of v_k^\perp . The energy gives an upper bound of the homogeneous $\dot{H}^{-1/2}$ -seminorm of the divergence $\nabla \cdot v_k$ in the regime $O(\frac{1}{|\log \eta_k|})$ and also, it has a fading control on the \dot{H}^1 -seminorm of v_k . Therefore, it is enough to estimate a perturbed homogeneous $\dot{H}^{1/2}$ -seminorm of χ_k by the total variation of χ_k . That holds true by the following localized version of a logarithmically failing interpolation inequality (see [7]) :

$$\int_{1 < |\xi| < 1/\eta_k} |\xi| |\mathcal{F}(\chi_k)|^2 d\xi \leq \frac{2}{\pi} |\log \eta_k| \sup |\chi_k| \int |\nabla \chi_k| dx.$$

9 Appendix

We compute the stray field energy for x_3 -invariant magnetizations in the general 3-D model. Let $\Omega = \Omega' \times (0, t)$, $\Omega' \subset \mathbb{R}^2$ be a bounded simply connected domain with Lipschitz boundary and $m = (m', m_3) : \Omega \rightarrow \mathbb{R}^3$. We extend m by 0 outside the domain Ω , so that we will always identify

$$m = m1_\Omega.$$

The stray field potential $U : \mathbb{R}^3 \rightarrow \mathbb{R}$ is the solution of the transmission problem (2) :

$$\begin{cases} \Delta U = \nabla \cdot m & \text{in } \Omega, \\ \Delta U = 0 & \text{in } \mathbb{R}^3 \setminus \Omega, \\ [U] = 0 & \text{on } \partial\Omega, \\ \left[\frac{\partial U}{\partial \nu} \right] = m \cdot \nu & \text{on } \partial\Omega, \end{cases} \quad (36)$$

where $[h] = h^+ - h^-$ stands for the jump of a quantity h with respect to the outer unit normal vector ν on $\partial\Omega$. If $m \in L^2(\Omega)$ and the normal trace $m \cdot \nu$ belongs to $H^{-1/2}(\partial\Omega)$, problem (36) has a unique solution in the Beppo-Levi space (see Dautray and Lions [6]) :

$$\mathcal{BL} = \{U : \mathbb{R}^3 \rightarrow \mathbb{R} : \nabla U \in L^2(\mathbb{R}^3), \frac{U}{1+|x|} \in L^2(\mathbb{R}^3)\}.$$

In fact, ∇U is the Helmholtz projection onto gradient fields of the magnetization m in the L^2 -topology and the potential U is fixed by the decay condition $U/(1+|x|) \in L^2$.

From now on, we assume that m does not depend on x_3 :

$$m = (m', m_3)(x').$$

The following formula holds for the stray field energy (see also DeSimone, Kohn, Müller and Otto [10] or Alouges and Labbé[1]) :

Proposition 1 *If m is x_3 -invariant in Ω , then*

$$\int_{\mathbb{R}^3} |\nabla U|^2 dx = t \int_{\mathbb{R}^2} f\left(\frac{t}{2}|\xi'|\right) \left| \frac{\xi'}{|\xi'|} \cdot \mathcal{F}(m'1_{\Omega'}) \right|^2 d\xi' + t \int_{\mathbb{R}^2} g\left(\frac{t}{2}|\xi'|\right) |\mathcal{F}(m_31_{\Omega'})|^2 d\xi',$$

where

$$g(s) = \frac{1 - e^{-2s}}{2s} \quad \text{and} \quad f(s) = 1 - g(s) \quad \text{if } s \geq 0.$$

Proof. Indeed, the Fourier transform $\mathcal{F}(U)(\xi', x_3)$ in the in-plane variables x' turns (36) into a second order ODE in the vertical variable x_3 for the wave number ξ' as a parameter :

$$\frac{\partial^2}{\partial x_3^2} \mathcal{F}(U)(\xi', x_3) - |\xi'|^2 \mathcal{F}(U)(\xi', x_3) = \begin{cases} 0 & \text{if } x_3 < 0 \text{ or } x_3 > t, \\ \mathcal{F}(\nabla' \cdot m')(\xi') & \text{if } x_3 \in (0, t), \end{cases}$$

with the boundary conditions

$$[\mathcal{F}(U)](\xi', 0) = [\mathcal{F}(U)](\xi', t) = 0 \quad \text{and} \quad \left[\frac{\partial}{\partial x_3} \mathcal{F}(U) \right](\xi', 0) = \left[-\frac{\partial}{\partial x_3} \mathcal{F}(U) \right](\xi', t) = \mathcal{F}(m_31_{\Omega'}) (\xi').$$

The solution is given by

$$\mathcal{F}(U)(\xi, x_3) = \begin{cases} \alpha(\xi') (e^{|\xi'|(x_3-t)} - e^{|\xi'|x_3}) & \text{if } x_3 < 0, \\ \beta(\xi') e^{-|\xi'|x_3} + \alpha(\xi') e^{|\xi'|(x_3-t)} - \frac{\mathcal{F}(\nabla' \cdot m')(\xi')}{|\xi'|^2} & \text{if } x_3 \in (0, t), \\ \beta(\xi') (e^{-|\xi'|x_3} - e^{|\xi'|(t-x_3)}) & \text{if } x_3 > t, \end{cases}$$

where

$$\alpha(\xi') = \frac{\mathcal{F}(\nabla' \cdot m')(\xi')}{2|\xi'|^2} + \frac{\mathcal{F}(m_3)(\xi')}{2|\xi'|} \quad \text{and} \quad \beta(\xi') = \frac{\mathcal{F}(\nabla' \cdot m')(\xi')}{2|\xi'|^2} - \frac{\mathcal{F}(m_3)(\xi')}{2|\xi'|}.$$

Therefore, Plancherel's identity leads to

$$\int_{\mathbb{R}^3} |\nabla U|^2 dx = \int_{\mathbb{R}} \int_{\mathbb{R}^2} \left(\left| \frac{\partial \mathcal{F}(U)}{\partial x_3} \right|^2 + |\xi'|^2 |\mathcal{F}(U)|^2 \right) d\xi' dx_3 = I_1 + I_2 + I_3$$

where

$$I_1 = \int_{-\infty}^0 \int_{\mathbb{R}^2} \left(\left| \frac{\partial \mathcal{F}(U)}{\partial x_3} \right|^2 + |\xi'|^2 |\mathcal{F}(U)|^2 \right) d\xi' dx_3 = \int_{\mathbb{R}^2} |\xi'| \alpha(\xi')^2 (1 - e^{-|\xi'|t})^2 d\xi',$$

$$\begin{aligned} I_2 &= \int_0^t \int_{\mathbb{R}^2} \left(\left| \frac{\partial \mathcal{F}(U)}{\partial x_3} \right|^2 + |\xi'|^2 |\mathcal{F}(U)|^2 \right) d\xi' dx_3 \\ &= \int_{\mathbb{R}^2} \left(|\xi'| (\alpha(\xi')^2 + \beta(\xi')^2) (1 - e^{-2|\xi'|t}) - 2(\alpha(\xi') + \beta(\xi')) (1 - e^{-|\xi'|t}) \frac{\mathcal{F}(\nabla' \cdot m')(\xi')}{|\xi'|} \right) d\xi' + \\ &\quad \int_{\mathbb{R}^2} t \frac{(\mathcal{F}(\nabla' \cdot m')(\xi'))^2}{|\xi'|^2} d\xi' \end{aligned}$$

and

$$I_3 = \int_t^\infty \int_{\mathbb{R}^2} \left(\left| \frac{\partial \mathcal{F}(U)}{\partial x_3} \right|^2 + |\xi'|^2 |\mathcal{F}(U)|^2 \right) d\xi' dx_3 = \int_{\mathbb{R}^2} |\xi'| \beta(\xi')^2 (1 - e^{-|\xi'|t})^2 d\xi'.$$

The conclusion is now straightforward. \square

Acknowledgments. The author thanks to B. Merlet and C. Melcher for useful comments on the paper.

Références

- [1] F. Alouges and S. Labbé, *z-invariant micromagnetic configurations in cylindrical domains*, preprint.
- [2] F. Alouges, T. Rivière and S. Serfaty, *Néel and cross-tie wall energies for planar micromagnetic configurations*, ESAIM Control Optim. Calc. Var. **8** (2002), 31–68.
- [3] L. Ambrosio, C. De Lellis and C. Mantegazza, *Line energies for gradient vector fields in the plane*, Calc. Var. Partial Differential Equations **9** (1999), 327–355.
- [4] P. Aviles and Y. Giga, *A mathematical problem related to the physical theory of liquid crystal configurations*, Proc. Centre Math. Anal. Austral. Nat. Univ. **12** (1987), 1–16.
- [5] F. Bethuel, H. Brezis and F. Hélein, *Ginzburg-Landau vortices*, Progress in Nonlinear Differential Equations and their Applications, 13. Birkhäuser Boston, Inc., Boston, MA, 1994.
- [6] R. Dautray and J.-L. Lions, *Analyse mathématique et calcul numérique pour les sciences et les techniques. Vol. 6*, Méthodes intégrales et numériques. [Integral and numerical methods], Masson, Paris 1988.
- [7] A. DeSimone, H. Knüpfer and F. Otto, *2-d stability of the Néel wall*, Calc. Var. Partial Differential Equations **27** (2006), 233–253.
- [8] A. Desimone, R. V. Kohn, S. Müller and F. Otto, *Magnetic microstructures—a paradigm of multiscale problems*, In ICIAM 99 (Edinburgh), pages 175–190. Oxford Univ. Press, Oxford, 2000.

- [9] A. DeSimone, R. V. Kohn, S. Müller and F. Otto, *A compactness result in the gradient theory of phase transitions*, Proc. Roy. Soc. Edinburgh **131** (2001), 833-844.
- [10] A. Desimone, R. V. Kohn, S. Müller and F. Otto, *A reduced theory for thin-film micromagnetics*, Comm. Pure Appl. Math. **55** (2002), 1408-1460.
- [11] A. Desimone, R. V. Kohn, S. Müller and F. Otto, *Repulsive interaction of Néel walls, and the internal length scale of the cross-tie wall*, Multiscale Model. Simul. **1** (2003), 57-104.
- [12] A. DeSimone, R. V. Kohn, S. Müller and F. Otto, *Recent analytical developments in micromagnetics*, in : Science of Hysteresis, Elsevier, G. Bertotti and I Magyergyoz, Eds., 2005.
- [13] A. DeSimone, R. V. Kohn, S. Müller, F. Otto and R. Schäfer, *Two-dimensional modelling of soft ferromagnetic films*, R. Soc. Lond. Proc. Ser. A Math. Phys. Eng. Sci. **457** (2001), 2983-2991.
- [14] C.J. García-Cervera, *Magnetic domains and magnetic domain walls*, Ph.D. thesis, New-York University (1999).
- [15] A. Hubert and R. Schäfer, *Magnetic domains*, Springer, 1998.
- [16] R. Ignat, *A Γ -convergence result for the Néel wall*, preprint.
- [17] R. Ignat and F. Otto, *A compactness result in thin-film micromagnetics and the optimality of the Néel wall*, J. Eur. Math. Soc. (JEMS), to appear.
- [18] R. Ignat and F. Otto, *Compactness of the Landau state in thin-film micromagnetics*, in preparation.
- [19] R. L. Jerrard, *Lower bounds for generalized Ginzburg-Landau functionals*, SIAM J. Math. Anal. **30** (1999), 721-746.
- [20] W. Jin and R. Kohn, *Singular perturbation and the energy of folds*. J. Nonlinear Sci. **10** (2000), 355-390.
- [21] F. Lin, *Vortex dynamics for the nonlinear wave equation*, Comm. Pure Appl. Math. **52** (1999), 737-761.
- [22] C. Melcher, *The logarithmic tail of Néel walls*, Arch. Ration. Mech. Anal. **168** (2003), 83-113.
- [23] C. Melcher, *Logarithmic lower bounds for Néel walls*, Calc. Var. Partial Differential Equations **21** (2004), 209-219.
- [24] F. Pacard and T. Rivière, *Linear and nonlinear aspects of vortices*, Progress in Nonlinear Differential Equations and their Applications, 39, Birkhäuser Boston Inc., Boston, MA, 2000.
- [25] R. Riedel and A. Seeger, *Micromagnetic treatment of Néel walls*, Phys. Stat. Sol. **46**, 1971, 377-384.
- [26] T. Rivière and S. Serfaty, *Limiting domain wall energy for a problem related to micromagnetics*, Comm. Pure Appl. Math. **54** (2001), 294-338.
- [27] T. Rivière and S. Serfaty, *Compactness, kinetic formulation, and entropies for a problem related to micromagnetics*, Comm. Partial Differential Equations **28** (2003), 249-269.
- [28] E. Sandier, *Lower bounds for the energy of unit vector fields and applications*, J. Funct. Anal. **152** (1998), 379-403.
- [29] H.A.M. van den Berg, *Self-consistent domain theory in soft-ferromagnetic media. II, Basic domain structures in thin film objects*, J. Appl. Phys. **60** (1986), 1104-1113.